Applied and Environmental Microbiology

Direct Conversion of Xylan to Ethanol by Recombinant Saccharomyces cerevisiae Strains Displaying an Engineered Minihemicellulosome

Jie Sun, Fei Wen, Tong Si, Jian-He Xu and Huimin Zhao
Appl. Environ. Microbiol. **2012, 78(11):3837. DOI: 10.1128/AEM.07679-11.**
Published Ahead of Print 23 March 2012.

AEM
Journals.ASM.org

Direct Conversion of Xylan to Ethanol by Recombinant *Saccharomyces cerevisiae* Strains Displaying an Engineered Minihemicellulosome

Jie Sun,[a,b] Fei Wen,[a] Tong Si,[a] Jian-He Xu,[b] and Huimin Zhao[a,c]

Department of Chemical and Biomolecular Engineering, University of Illinois at Urbana-Champaign, Urbana, Illinois, USA[a]; State Key Laboratory of Bioreactor Engineering, East China University of Science and Technology, Shanghai, China[b]; and Departments of Chemistry, Biochemistry, and Bioengineering, Institute for Genomic Biology, Center for Biophysics and Computational Biology, University of Illinois at Urbana-Champaign, Urbana, Illinois, USA[c]

Arabinoxylan is a heteropolymeric chain of a β-1,4-linked xylose backbone substituted with arabinose residues, representing a principal component of plant cell walls. Here we developed recombinant *Saccharomyces cerevisiae* strains as whole-cell biocatalysts capable of combining hemicellulase production, xylan hydrolysis, and hydrolysate fermentation into a single step. These strains displayed a series of uni-, bi-, and trifunctional minihemicellulosomes that consisted of a miniscaffoldin (CipA3/CipA1) and up to three chimeric enzymes. The miniscaffoldin derived from *Clostridium thermocellum* contained one or three cohesin modules and was tethered to the cell surface through the *S. cerevisiae* a-agglutinin adhesion receptor. Up to three types of hemicellulases, an endoxylanase (XynII), an arabinofuranosidase (AbfB), and a β-xylosidase (XlnD), each bearing a C-terminal dockerin, were assembled onto the miniscaffoldin by high-affinity cohesin-dockerin interactions. Compared to uni- and bifunctional minihemicellulosomes, the resulting quaternary trifunctional complexes exhibited an enhanced rate of hydrolysis of arabinoxylan. Furthermore, with an integrated D-xylose-utilizing pathway, the recombinant yeast displaying the bifunctional minihemicellulosome CipA3-XynII-XlnD could simultaneously hydrolyze and ferment birchwood xylan to ethanol with a yield of 0.31 g per g of sugar consumed.

Liquid biofuels, such as bioethanol, are derived mainly from grain or sugarcane and are generally considered a sustainable solution to many energy and environmental problems (18, 42, 43, 50). However, the diversity and recalcitrant structure of lignocellulose together with other bottlenecks, such as the large amounts of various enzymes required, inefficient lignocellulosic hydrolysis, and incomplete fermentation, have impeded the development of biofuels (16, 23). One potential strategy to overcome these limitations is consolidated bioprocessing (CBP), which combines enzyme production, hydrolysis, and fermentation in one step. In this strategy, a single microorganism capable of fermenting pretreated biomass without added lignocellulolytic enzymes is required, which could potentially result in a lower cost of production of lignocellulosic ethanol (27, 48).

Previously, we engineered a recombinant *Saccharomyces cerevisiae* strain displaying a trifunctional minicellulosome that could directly ferment phosphoric acid-swollen cellulose to ethanol with a titer of ~1.8 g/liter (51). Here we target the second most abundant polysaccharide (hemicellulose [β-1,4-xylan]), representing 15 to 35% of various lignocelluloses (38), to examine if we could incorporate hemicellulase function in a scaffoldin format, thereby yielding a "minihemicellulosome." Arabinoxylan is a major component of the plant cell wall, especially in cereal grains such as wheat and rice (10). The minimum enzymatic combination to hydrolyze arabinoxylan into xylose includes an endo-1,4-β-xylanase (EC 3.2.1.8), which hydrolyzes xylan into xylooligosaccharides; a β-xylosidase (EC 3.2.1.37), which hydrolyzes xylooligosaccharides into D-xylose; and an α-L-arabinofuranosidase (EC 3.2.1.55), which cleaves arabinose side residues that restrict the access of endoxylanase and xylosidase to the xylosidic linkage in the backbone (10, 42). Hemicellulases are produced mainly by two fungi, *Trichoderma reesei* and *Aspergillus niger*, on an industrial scale (1). Most of them have been heterologously expressed in *S. cerevisiae* (38, 48). For example, the endoxylanase XynII from *T. reesei* showed a high activity of 72 U/ml toward birchwood glucuronoxylan and retained an activity of 52 U/ml when coexpressed with the xylosidase XlnD from *A. niger* (24, 25). In addition, several α-L-arabinofuranosidases have been cloned from these two fungi and expressed in *S. cerevisiae*, such as AbfB (*A. niger*) (1.4 U/ml) (9) and Abf1 (*T. reesei*) (0.21 U/ml) (29). Two β-xylosidases have been cloned from *T. reesei* (Bxl1 [0.02 U/ml]) (29) and *A. niger* (XlnD [0.32 U/ml]) (24). We chose the three best-characterized hemicellulases, *T. reesei* XynII, *A. niger* AbfB, and *A. niger* XlnD, as the main catalytic components in the engineered minihemicellulosomes.

The cellulosome, a multienzyme complex that contains a noncatalytic scaffoldin protein and several dockerin-bearing catalytic modules, was initially discovered in the thermophilic anaerobic bacterium *Clostridium thermocellum* (2, 6). Such an extracellular supermachine can harbor cellulases by cohesin-dockerin interactions and enable the conversion of lignocellulose to microbial cell mass and products simultaneously (3). Compared to a noncomplexed system, which secretes free enzymes, this complexed system can control the incorporation of enzyme components that act synergistically. Recently, there has been increasing interest in the

Received 24 November 2011 **Accepted** 15 March 2012
Published ahead of print 23 March 2012
Address correspondence to Huimin Zhao, zhao5@illinois.edu.
Supplemental material for this article may be found at http://aem.asm.org/.

doi:10.1128/AEM.07679-11

TABLE 1 Characteristics of recombinant yeast strains used in this study

Strain	Plasmid(s)	Relevant feature(s)
S. cerevisiae EBY100		
HZ1901[a]	pYDctrl and pRS425	No surface display (control strain)
HZ2216 (CipA3-XynII)	pYD1-CipA3-XynII	Displays unifunctional minihemicellulosome with XynII activity
HZ1931 (CipA3-AbfB)	pYD1-CipA3[a] and pRS425-AbfB	Displays unifunctional minihemicellulosome with AbfB activity
HZ1933 (CipA3-XlnD)	pYD1-CipA3 and pRS425-XlnD	Displays unifunctional minihemicellulosome with XlnD activity
HZ3358 (CipA3-XynII-AbfB)	pYD1-CipA3-XynII and pRS425-AbfB	Displays bifunctional minihemicellulosome with XynII and AbfB activities
HZ3361 (CipA3-XynII-XlnD)	pYD1-CipA3-XynII and pRS425-XlnD	Displays bifunctional minihemicellulosome with XynII and XlnD activities
HZ3355 (CipA3-XynII-AbfB-XlnD)	pYD1-CipA3-XynII and pRS425-AbfB-XlnD	Displays trifunctional minihemicellulosome with XynII, AbfB, and XlnD activities
HZ3376 (CipA1-XynII)	pYD1-CipA1-XynII	Displays one type of unifunctional minihemicellulosome with XynII activity
HZ3370 (CipA1-XynII-AbfB)	pYD1-CipA1-XynII and pRS425-AbfB	Displays two types of unifunctional minihemicellulosomes, with XynII and AbfB activities, respectively
HZ3373 (CipA1-XynII-XlnD)	pYD1-CipA1-XynII and pRS425-XlnD	Displays two types of unifunctional minihemicellulosomes, with XynII and XlnD activities, respectively
HZ3367 (CipA1-XynII-AbfB-XlnD)	pYD1-CipA1-XynII and pRS425-AbfB-XlnD	Displays three types of unifunctional minihemicellulosomes, with XynII, AbfB, and XlnD activities, respectively
S. cerevisiae L2612		
HZ3345 (CipA3-XynII-XlnD)	pYD1-CipA3-XynII and pRS425-XlnD	Displays bifunctional minihemicellulosome with XynII and XlnD activities on strain HZ3001
HZ3001[b]		Integrated with a xylose-utilizing pathway from *S. stipitis* on the chromosome of *S. cerevisiae* L2612

[a] See reference 51.
[b] See reference 26.

heterologous expression of cellulosomes and assembly in a Lego-like way so that functional cellulosomes could be formed either *in vivo* or *in vitro* (8, 13, 19, 31, 39, 47, 51). However, little attention has been paid to the heterologous expression of hemicellulosomes, which are also produced naturally by some bacteria (20, 22). Kondo and coworkers previously constructed a xylan-fermenting yeast strain by codisplaying hemicellulases on the surface of xylose-utilizing *S. cerevisiae* cells but did not use a scaffoldin (14, 21). More recently, Bayer and coworkers used a designer cellulosome approach (4) to construct hemicellulosomes *in vitro* by assembling four xylanases into defined artificial cellulosome complexes and showed that the resulting tetravalent xylanolytic designer cellulosomes displayed enhanced activities on untreated natural wheat straw compared to wild-type free-xylanase systems (32–34).

Here we report the construction of a trifunctional minihemicellulosome on the yeast cell surface. The chimeric enzymes could be assembled *in vivo* on the miniscaffoldin to hydrolyze arabinoxylan into D-xylose and arabinose. To further enable *S. cerevisiae* to utilize D-xylose, the known D-xylose utilization pathway consisting of xylose reductase (XR), xylitol dehydrogenase (XDH), and D-xylulokinase (XK) from *Scheffersomyces stipitis* was integrated into the *S. cerevisiae* L2612 genome as described previously (26, 44). Direct conversion from birchwood xylan to ethanol was achieved after incorporating the bifunctional minihemicellulosome into our engineered D-xylose-utilizing *S. cerevisiae* strain L2612.

MATERIALS AND METHODS

Strains, media, and reagents. *S. cerevisiae* EBY100 (Invitrogen, Carlsbad, CA) was used for yeast cell surface display. *Escherichia coli* DH5α (Cell Media Facility, University of Illinois at Urbana-Champaign, Urbana, IL) was used for recombinant DNA manipulation. *Trichoderma reesei* DSM769 and *Aspergillus niger* DSM821 were purchased from the DSMZ (Braunschweig, Germany). *T. reesei* and *A. niger* were grown on YPAX media (1% yeast extract, 2% peptone, 0.01% adenine hemisulfate, 2% birchwood xylan) to form spores. The cDNA was synthesized from mRNA by using the First-Strand cDNA synthesis kit (Roche, Indianapolis, IN). Recombinant *S. cerevisiae* EBY100 transformants were selected and maintained on synthetic complete (SC) dropout medium, SC medium lacking Trp (SC−Trp medium), SC−Leu, SC−Trp−Leu, or SC−Trp−Leu−Ura, which contains 0.167% yeast nitrogen base without amino acids and ammonium sulfate (Difco Laboratories, Detroit, MI), 0.5% ammonium sulfate, 2% glucose, and appropriate supplements (with 1.5% agar added for solid plates). YPG (1% yeast extract, 2% peptone, 2% galactose) was used to induce protein expression in yeast cells. *E. coli* was cultured in LB medium (Fisher, Pittsburgh, PA). The substrates, arabinoxylan (catalog number P-WAXYM) and xylooligosaccharides (xylobiose, xylotriose, and xylotetraose), were purchased from Megazyme (Bray Co., Wicklow, Ireland). The preparation of the arabinoxylan solution was carried out according to the manufacturer's instructions. The substrate birchwood xylan (catalog number X0502) and all the other chemicals were obtained from Sigma (St. Louis, MO). All restriction enzymes were purchased from New England BioLabs (Ipswich, MA).

Plasmid construction. The features of all the recombinant *S. cerevisiae* strains are listed in Table 1. The sequences of all PCR primers used are summarized in Table S1 in the supplemental material, while the corresponding PCR products, templates, and primer pairs used are shown in Table S2 in the supplemental material. The endo-1,4-β-xylanase (XynII) was amplified from *T. reesei* cDNA by PCR using primer pair His-Xyn2For/His-Xyn2Rev, and the PCR product His-Xyn2-HR was cotransformed with BclI-digested pRS425-EGII (51), yielding plasmid pRS425-XynII. Plasmids pYD1-CipA3-XynII and pYD1-CipA1-XynII were constructed by cotransforming Xyn2-ind-HR with SacI-linearized pYD1-

CipA3-EGII (51) and pYD1-CipA1-EGII (51), respectively, into EBY100. The genes encoding α-L-arabinofuranosidase (AbfB) and β-xylosidase (XlnD) were obtained by PCR using cDNA of *A. niger* as the template and primer pairs FLAG-abfBFor/FLAG-abfBRev and c-Myc-xlnDFor/c-Myc-xlnDRev, respectively. The resulting PCR products, FLAG-abfB-HR and c-Myc-xlnD-HR, were cotransformed with BclI-digested pRS425-CBHII (51) and BamHI-digested pRS425-BGLI (51), respectively, yielding plasmids pRS425-AbfB and pRS425-XlnD, respectively. Plasmid pRS425-AbfB-XlnD was obtained by cotransforming XdAb-HR2, XdAb-ind-HR, and ApaI-digested pRS425-XlnD into EBY100. The construction of all plasmids involved a conventional homologous recombination method (28). All the plasmids were verified by DNA sequencing.

Strain HZ3001 was previously created by integrating the D-xylose-utilizing pathway from *S. stipitis*, including xylose reductase (XR), xylitol dehydrogenase (XDH), and D-xylulokinase (XK), into *S. cerevisiae* L2612 (26). Three individual cassettes, *hisG-ADH1p-XR-ADH1t*, *PGK1p-XDH-CYC1t*, and *PYK1p-XKS-ADH2t*-δ*2*, were assembled by overlap extension PCR (OE-PCR), purified, and mixed with the BamHI/XhoI-digested integration fragment δ*1-hisG-ura3-hisG*, which carries a *ura3* selection marker and a δ sequence that shares sequence identity to the partial sequence of δ sites on the yeast chromosome (44). Xylan-utilizing strain HZ3345 was then obtained by cotransforming pYD1-CipA3-XynII and pRS425-XlnD into this strain (Table 1).

Yeast surface display and flow cytometry analysis. *S. cerevisiae* EBY100 transformants were cultured in SC dropout medium for 1 day. The cell pellets were then washed with YPG medium three times and induced in YPG medium for 48 h at 20°C at 250 rpm. Each staining assay was performed with 2.5×10^6 cells. Anti-V5 (Invitrogen), anti-His (Sigma), anti-FLAG (Sigma), and anti-c-Myc (Invitrogen) antibodies were used as the primary monoclonal antibodies. The levels of surface expression of miniscaffoldin and xylanases were analyzed by flow cytometry and expressed as relative mean fluorescence units, as described elsewhere previously (51).

Enzyme activity assays. The xylanase-producing yeast strains were cultured in SC dropout medium and induced in YPG medium. Arabinoxylan was used to analyze the activity of XynII. After centrifugation, the cells were washed three times with reaction buffer (50 mM potassium acetate buffer, pH 5.0) to prevent medium carryover and then resuspended in reaction buffer supplemented with 0.1% arabinoxylan to an optical density at 600 nm (OD_{600}) of ~1. The reaction was carried out at 30°C at 250 rpm. Samples of 1 ml were taken at the time intervals indicated. The amount of reducing sugar released from arabinoxylan was measured by using the Somogyi-Nelson method as described elsewhere previously (52).

The activity of AbfB was measured by using 4-nitrophenyl α-L-arabinofuranoside (4NPAF). The recombinant yeast cells were first washed three times and resuspended in reaction buffer (50 mM sodium phosphate, 100 mM NaCl [pH 5.0]) with 1 mM 4NPAF to an OD_{600} of ~1. After incubation at 30°C at 250 rpm, 1-ml samples were centrifuged at the time intervals indicated, and the supernatants were terminated by the addition of a 1:2 (vol/vol) volume of 1 M Na_2CO_3. The absorbance of released 4-nitrophenyl (4NP) was measured at 405 nm and quantified by using 4NP standards.

The activity of XlnD was determined by hydrolyzing 0.1% xylooligosaccharides (xylobiose [X2], xylotriose [X3], and xylotetraose [X4]) in 50 mM potassium acetate buffer at pH 5.0. The cell density in the reaction medium was adjusted to an OD_{600} of ~1. The reaction was performed at 30°C at 250 rpm. Samples were centrifuged and filtered through a 0.22-μm polyethersulfone filter (Corning, Lowell, MA) at the indicated time intervals to analyze the concentrations of xylose, xylobiose, xylotriose, and xylotetraose. The analysis was performed by using a Shimadzu high-performance liquid chromatography (HPLC) instrument equipped with a RID-10A refractive index detector (Shimadzu, Columbia, MD). The separation of xylooligosaccharides was carried out by using an Aminex HPX-87H column (Bio-Rad, Philadelphia, PA). The operation conditions were 65°C using a mobile phase of 50 mM H_2SO_4 at 0.6 ml/min.

Hydrolysis of xylan. Yeast transformants displaying different minihemicellulosomes were analyzed for their abilities to hydrolyze xylan. After induction in YPG medium, cells were washed with hydrolysis buffer (50 mM potassium acetate buffer, pH 5.0) three times and resuspended with 1% (wt/vol) arabinoxylan or 0.1% (wt/vol) birchwood xylan to an OD_{600} of ~10. Hydrolysis reactions were carried out with serum bottles (Wheaton, Millville, NJ) at 30°C at 200 rpm. Samples of 1 ml were removed and analyzed by both the Somogyi-Nelson method and HPLC as described above. All sugar concentrations were determined as xylose equivalents.

Fermentation. Xylan-utilizing strain HZ3345 and control strain HZ3001 were precultivated in 30 ml SC dropout medium and induced with 60 ml YPG medium for 48 h at 20°C at 250 rpm. The cells were collected by centrifugation at 4,000 rpm for 10 min and washed three times with YP medium (1% yeast extract, 2% peptone). Cells were resuspended to an OD_{600} of ~50 with fermentation medium consisting of 1% yeast extract, 2% peptone, 1% birchwood xylan, 0.001% ergosterol, and 0.042% Tween 80. All the reagents and media were prepared in an anaerobic chamber after flushing with an anaerobic gas mixture and continually stirred for at least 1 week. Direct fermentation was carried out anaerobically in serum bottles at 30°C at 250 rpm. Samples of 1 ml were removed at the time intervals indicated. The residual total sugar concentration was determined by the phenol-sulfuric acid method (52) and calculated by subtracting the concentration of cell-derived sugar from the total sugar concentration of the culture. The ethanol concentration was measured by HPLC as described above.

RESULTS

Design of minihemicellulosomes. The bioconversion of xylan to monosaccharides (like xylose and arabinose) and other side residues requires the synergistic action of at least three types of xylanases (two main-chain cleavage enzymes and other side-chain cleavage enzymes) (40). For arabinoxylan, the enzyme arabinofuranosidase could cleave arabinose residues from substituted xylooligosaccharides to leave linear, nonbranched xylooligosaccharides (10). Hence, we designed minihemicellulosomes consisting of up to three enzymes, including a miniscaffoldin, an endoxylanase (XynII), an arabinofuranosidase (AbfB), and a β-xylosidase (XlnD). Two types of miniscaffoldin (mini-CipA), CipA3 and CipA1, were designed to contain either three (Coh1, Coh2, and Coh3) or one (Coh3) cohesin module isolated from the *C. thermocellum cipA* gene (15, 51). The cohesin domains in the *cipA* gene are numbered 1 to 9 in accordance with their positions from the N terminus (45). The N terminus of mini-CipA was fused to the AGA2 protein in the yeast pYD1 display vector (51). By the yeast a-agglutinin mating adhesion receptor, miniscaffoldins were expected to be displayed on the cell surface (Fig. 1).

Each chimeric hemicellulase construct consists of a promoter, a secretion signal peptide, an epitope tag, a target hemicellulase, a dockerin module, and a terminator. Specifically, they are designated GAL10-(prepro signal peptide)-His-XynII-docS-ADH1, GAL1-(α-factor signal peptide)-FLAG-AbfB-docS-ADH2, and GAL10–(prepro signal peptide)–c-Myc–XlnD–docA–ADH1, respectively. Since the enzymes AbfB and XlnD were expressed from a single vector, they were fused with two different dockerins to avoid potential plasmid instability issues due to long stretches of homology/identical sequences (35, 44). The two dockerin modules docS and docA were obtained from two major components in the cellulosome of *C. thermocellum*, CelS (49) and CelA (7). Since they are both type I dockerin domains, docS and docA can non-

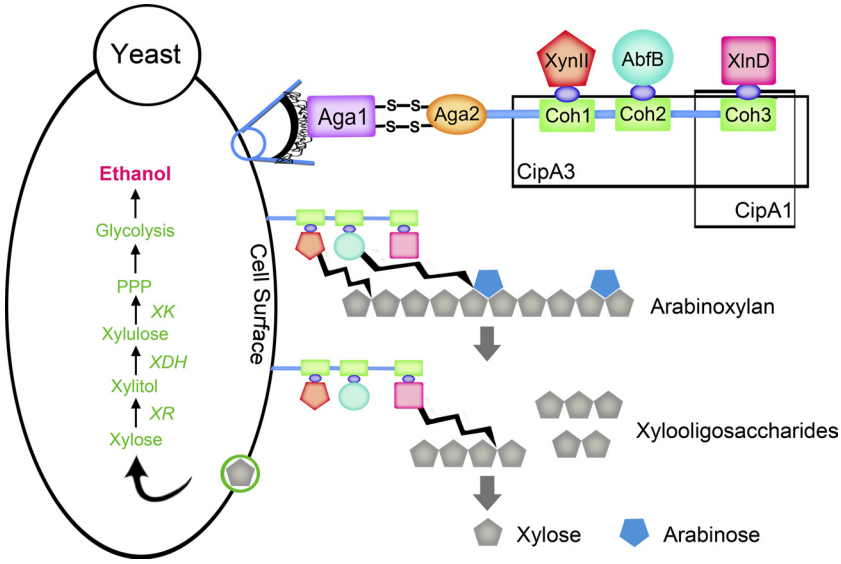

FIG 1 Design of a yeast surface display system for constructing minihemicellulosomes. The miniscaffoldins CipA3 and CipA1 contained three type I cohesin domains (Coh1, Coh2, and Coh3) and one type I cohesin domain (Coh3), respectively, and were tethered to the cell surface through Aga1-Aga2 interactions. Three hemicellulases, endoxylanase (XynII), arabinofuranosidase (AbfB), and xylosidase (XlnD), were displayed on the miniscaffoldin via the nonspecific type I cohesin-dockerin interaction. The figure shown assumes that the three hemicellulases are expressed at a 1:1:1 ratio. Theoretically, there are 27 possible configurations of trifunctional minihemicellulosomes, with three possibilities at each cohesin position. The D-xylose-utilizing pathway, including the xylose reductase (XR), xylitol dehydrogenase (XDH), and D-xylulokinase (XK) from *Scheffersomyces stipitis*, was integrated into the *S. cerevisiae* L2612 strain. The green-encircled gray pentagon on the cell surface shows that the released xylose is being transported into yeast cells. PPP, pentose phosphate pathway.

specifically interact with any type I cohesin domain (Coh1 to Coh3) in the scaffoldin CipA3/CipA1 (11). Four epitope tags, V5, His, FLAG, and c-Myc, were used for the detection of four components on the minihemicellulosomes. The chimeric enzymes His-XynII-docS, FLAG-AbfB-docS, and c-Myc–XlnD–docA were expected to be secreted and interact with the cohesin domains of the miniscaffoldin on the cell surface, forming a minihemicellulosome. The expression level of each component was then analyzed by detecting the protein expression tags by using flow cytometry. Note that each component was paired with one specific epitope tag.

Yeast surface display of uni-, bi-, and trifunctional hemicellulosomes. Since the scaffoldin was confirmed to be displayed on the yeast cell surface (51), unifunctional minihemicellulosomes were assembled to test the expression level of each individual enzyme. Plasmid pRS425 encoding one chimeric enzyme with or without plasmid pYD1-CipA3 was then transformed into yeast cells. The display level of each enzyme was monitored by measuring the corresponding protein expression tag using flow cytometry. As shown in Fig. 2A, the three chimeric enzymes were detected on the cell surface only when the scaffoldin CipA3 was coexpressed. Without CipA3, the enzyme was detected only in the supernatant, as determined by enzyme activity assays (see Fig. S1 in the supplemental material). The strains transformed with chimeric enzymes alone showed a small amount of nonspecific background fluorescence and no CipA3 expression (Fig. 2A). All of these results indicated that the unifunctional minihemicellulosomes were successfully assembled on the yeast cell surface through cohesin-dockerin interactions.

Bifunctional and trifunctional minihemicellulosomes were constructed by incorporating additional xylanases. Since XynII is the dominant enzyme to deconstruct xylan, bifunctional mini-

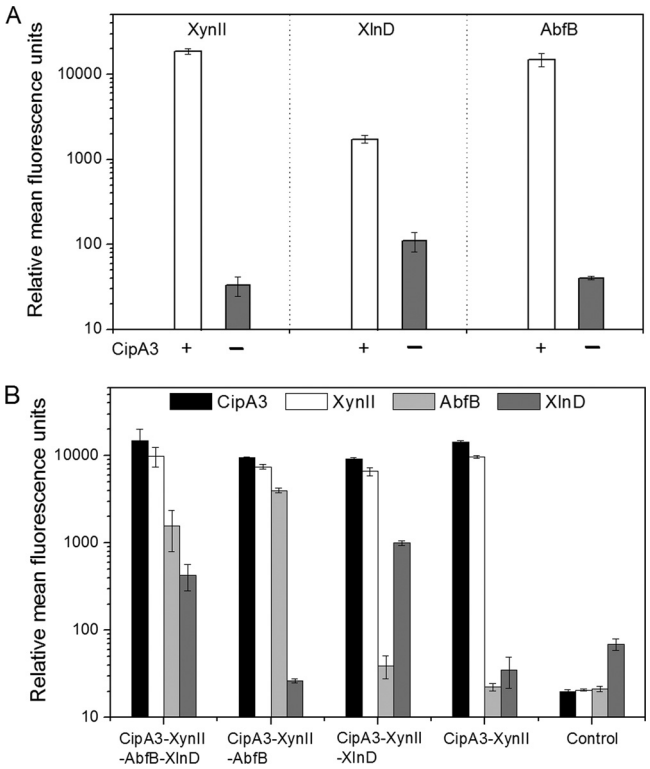

FIG 2 Yeast surface display levels of all CipA3-based minihemicellulosomal components. (A) Expression levels of enzymes in unifunctional minihemicellulosomes, including CipA3-XynII, CipA3-AbfB, and CipA3-XlnD. The blank columns represent the strains displaying CipA3 and a corresponding enzyme. The gray columns represent the strains displaying only a corresponding chimeric enzyme. (B) Expression levels of uni-, bi-, and trifunctional minihemicellulosomes. See Table 1 for the relevant features of each yeast strain. Relative mean fluorescence units of each component were obtained by flow cytometry. All the experiments were done in triplicate, and the averages and standard deviations are plotted.

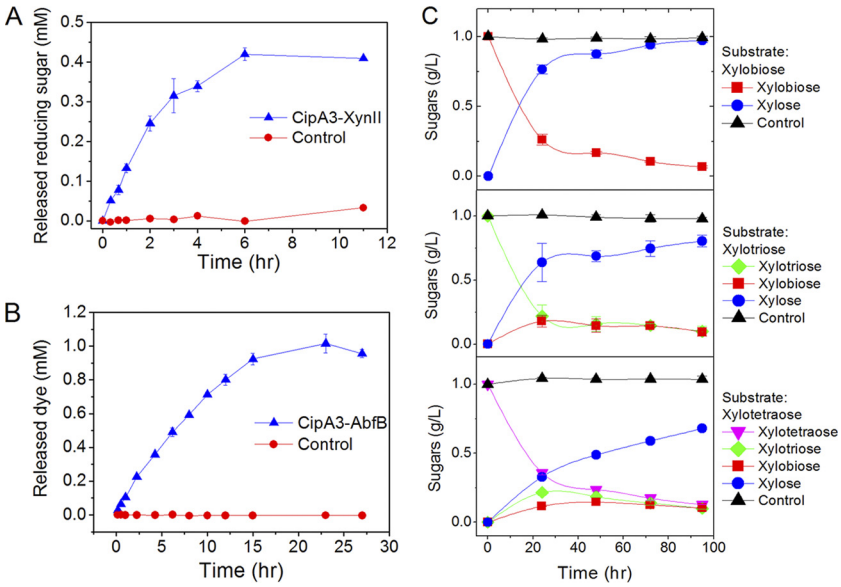

FIG 3 Functional analysis of three recombinant enzymes, XynII, AbfB, and XlnD. (A) Arabinoxylan hydrolysis activities were determined for cells displaying XynII. The reaction buffer used was 50 mM potassium acetate buffer (pH 5.0) supplemented with 0.1% arabinoxylan to an OD_{600} of ~1. (B) Cells displaying AbfB were assayed for their activities by the release of 4NP from the substrate 4NPAF. The reaction buffer used was 50 mM sodium phosphate–100 mM NaCl (pH 5.0) supplemented with 1 mM 4NPAF to an OD_{600} of ~1. (C) Time course of cells displaying XlnD to release sugars from xylooligosaccharides, including substrates of xylobiose (top), xylotriose (middle), and xylotetraose (bottom). The reaction buffer used was 50 mM potassium acetate (pH 5.0) supplemented with 0.1% xylooligosaccharides to an OD_{600} of ~1. Strain HZ1901 (Table 1) carrying two empty vectors, pYD1 and pRS425, was used as the negative control. All the experiments were performed at 30°C at 250 rpm and were done in triplicate. The averages and standard deviations are plotted.

hemicellulosomes were designed with XynII in combination with AbfB or XlnD, resulting in CipA3-XynII-AbfB and CipA3-XynII-XlnD (Table 1). The trifunctional minihemicellulosome is CipA3-XynII-AbfB-XlnD (Table 1). Compared to yeast strains displaying CipA3-XynII, CipA3-AbfB, or CipA3-XlnD, bifunctional minihemicellulosomes did not show significant decreases in display levels of any component (Fig. 2A and B). The addition of a third enzyme, XlnD, in the CipA3-XynII-AbfB-XlnD strain, however, did lead to decreased mean fluorescence units of AbfB and XlnD, by 2.54- and 2.35-fold, respectively (Fig. 2B). This might be due to the metabolic burden caused by the expression of four components simultaneously, which was also observed in a previous minicellulosome study (51). Nonetheless, these data clearly suggested that all the components of the minihemicellulosomes were successfully displayed on the cell surface. The cohesin-dockerin interaction was sufficient to direct the assembly of the quaternary minihemicellulosome.

Enzyme activities. The arabinoxylan that was used as the substrate contained 38% arabinose, 62% xylose, and trace amounts of other sugars, which represent the principal components of the plant cell wall, especially in rice bran, wheat arabinoxylan, and corn fiber (40). As shown in Fig. 3A, the recombinant yeast strain displaying XynII (CipA3-XynII) released 0.42 mM reducing sugars after 6 h, while no activity was detected in the control strain. The activity of AbfB was also examined by using the 4NPAF assay. As shown in Fig. 3B, the displayed AbfB enzyme could cleave the glycosidic bond of 4NPAF and liberate arabinose, as indicated by the detection of the coproduct 4NP. In contrast, the control strain did not show any activity toward the substrate 4NPAF.

The activity of XlnD was determined by using xylooligosaccharides with degrees of polymerization between 2 and 4 as the substrate. As shown in Fig. 3C, the strain displaying XlnD (CipA3-XlnD) showed activities toward all xylooligosaccharides tested. The higher the degree of polymerization of the substrate, the lower the amount of xylose released. Instead of being completely hydrolyzed into xylose, xylobiose was produced in the presence of xylotriose. Similarly, xylobiose and xylotriose were produced in the presence of xylotetraose. This corresponds to the mode of action of xylosidases, which release one monomer from the nonreducing end of xylooligosaccharides (10). The production of xylose from xylooligosaccharides was immediately observed without any lag phase. In addition, possible inhibition by the xylooligosaccharides was eliminated by incubation for a longer time, in which the substrates were eventually used up (data not shown). We conclude that XlnD is quite active in releasing xylose monomers in the final step of xylan degradation. No activity was detected in the control strain. Taken together, all three recombinant enzymes were shown to be active on the yeast cell surface. Of note, the binding efficiency of each enzyme was determined by an activity assay of the cell-associated enzyme and the corresponding enzyme in the supernatant. The display percentages of the enzymes XynII, AbfB, and XlnD were around 50%, 33%, and 53%, respectively (see Fig. S2 in the supplemental material).

Enhanced xylan conversion in minihemicellulosomes. The recombinant CipA3-based minihemicellulosomes were further evaluated for their abilities to hydrolyze arabinoxylan and birchwood xylan. Figure 4A represents the time course of reducing sugar released from arabinoxylan. HPLC analysis of the hydrolysis products showed that the CipA3-XynII strain released xylobiose and xylotriose as its main products, while only xylose was detected in the supernatant of the CipA3-XynII-XlnD strain (data not shown), indicating that both XynII and XlnD functioned effectively. The peak of arabinose was observed only for the CipA3-XynII-AbfB and CipA3-XynII-AbfB-XlnD strains (data not

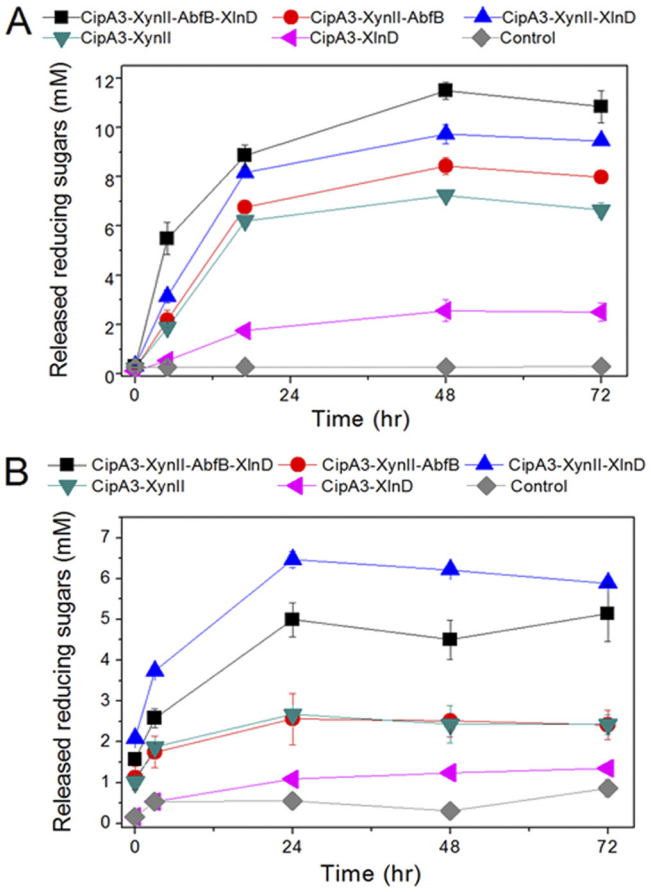

FIG 4 Functional analysis of surface-displayed CipA3-based minihemicellulosomes. (A) Hydrolysis of arabinoxylan from CipA3-based uni-, bi-, and trifunctional minihemicellulosomes. (B) Hydrolysis of birchwood xylan from CipA3-based uni-, bi-, and trifunctional minihemicellulosomes. The hydrolysis reactions were performed with 50 mM potassium acetate buffer (pH 5.0) with 1% (wt/vol) arabinoxylan or 0.1% (wt/vol) birchwood xylan to an OD_{600} of ~10. The experiments were carried out with serum bottles at 30°C at 200 rpm. All the experiments were done in triplicate, and the averages and standard deviations are plotted.

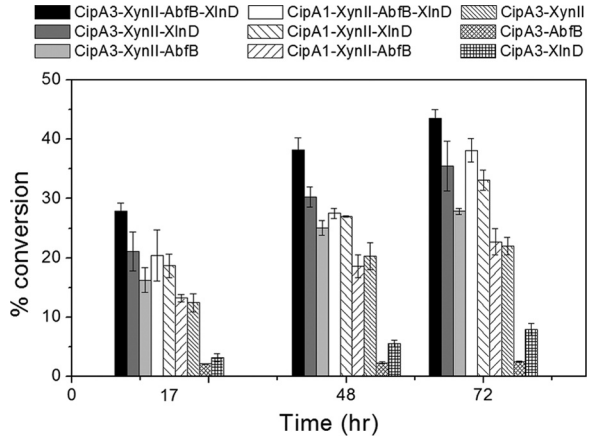

FIG 5 Percentages of arabinoxylan conversion for nine surface-engineered yeast strains were compared after 17 h, 48 h, and 72 h. The differences between CipA1-based minihemicellulosomes and the unifunctional CipA3-based minihemicellulosomes reflect enzyme-enzyme synergy. The differences between the CipA3-based and the corresponding CipA1-based minihemicellulosomes reflect enzyme proximity synergy.

shown). Both the HPLC analysis and the Somogyi-Nelson assay (Fig. 4A) showed that no arabinoxylan was hydrolyzed by the control strain.

In the case of arabinoxylan hydrolysis, a larger amount of reducing sugar was released by strains displaying the bifunctional and trifunctional minihemicellulosomes than by strains displaying the unifunctional minihemicellulosomes (CipA3-XynII and CipA3-XlnD) (Fig. 4A). The CipA3-XynII-AbfB, CipA3-XynII-XlnD, and CipA3-XynII-AbfB-XlnD strains could liberate reducing sugars of 7.24 mM, 9.73 mM, and 11.49 mM at 48 h, respectively. The bifunctional minihemicellulosomes (CipA3-XynII-AbfB and CipA3-XynII-XlnD) showed a higher rate of arabinoxylan hydrolysis than the unifunctional minihemicellulosomes, while the trifunctional minihemicellulosome (CipA3-XynII-AbfB-XlnD) showed the highest hydrolysis rate. The maximum amount of released reducing sugar was observed after ~48 h (Fig. 4A), and afterwards, it was slightly decreased and remained steady after ~3 days (data not shown). An interesting phenomenon was found in the case of the substrate birchwood xylan (Fig. 4B), which contains fewer substitutions of arabinose than arabinoxylan. The CipA3-XynII-XlnD strain exhibited a higher hydrolysis rate than the CipA3-XynII-AbfB-XlnD strain, while the CipA3-XynII-AbfB and CipA3-XynII strains showed very similar hydrolysis profiles. Therefore, the enzyme AbfB did not improve the hydrolytic performance of the enzymes XynII and XlnD on birchwood xylan.

Another scaffoldin, CipA1, containing only one cohesin module (Coh3), was designed to construct the CipA1-XynII, CipA1-XynII-AbfB, CipA1-XynII-XlnD, and CipA1-XynII-AbfB-XlnD strains (Fig. 1 and Table 1). The expression level of each component in CipA1-based minihemicellulosomes was similar to that in the corresponding CipA3-based minihemicellulosomes (see Fig. S3 in the supplemental material), which eliminated the effect of gene expression variation. CipA1 allows the simultaneous display of two or three types of unifunctional minihemicellulosomes on the cell surface (Fig. 1). As shown in Fig. 5, the CipA1-XynII-XlnD and CipA1-XynII-AbfB-XlnD strains both showed ~1.33-, ~4.88-, and ~11.74-fold-higher activities than the CipA3-XynII, CipA3-XlnD, and CipA3-AbfB strains at 48 h, respectively. Furthermore, when enzymes were brought into proximity on the miniscaffoldin, the CipA3-XynII-XlnD and CipA3-XynII-AbfB-XlnD strains additionally showed ~1.12- and ~1.39-fold-higher activities than the corresponding CipA1 strains, respectively. Notably, AbfB showed enzyme-enzyme synergy only after being brought in proximity to XynII and XlnD on CipA3 rather than on CipA1. The CipA1-XynII-XlnD and CipA1-XynII-AbfB-XlnD strains showed almost identical time course curves of released reducing sugar from arabinoxylan (data not shown), while an obvious improvement was observed for the corresponding CipA3 strains (Fig. 4A and 5).

Direct fermentation. To enable the yeast strain to utilize xylose, a D-xylose-utilizing pathway was integrated into the chromosome of *S. cerevisiae* L2612, yielding strain HZ3001 (Table 1). Since the substrate birchwood xylan contains >90% xylose residues, a bifunctional minihemicellulosome, CipA3-XynII-XlnD, was displayed on the surface of strain HZ3001, yielding strain HZ3345 (Table 1). Both strains were first tested for their growth

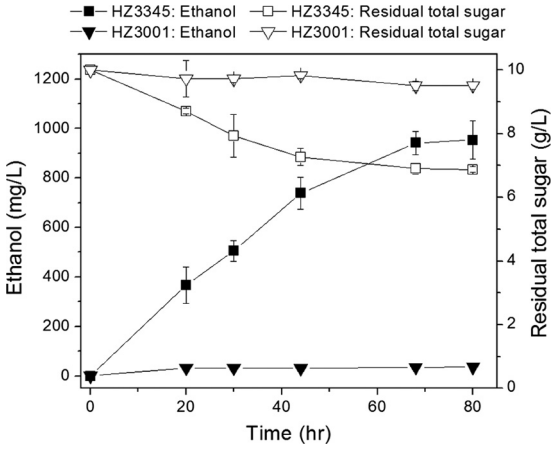

FIG 6 Direct fermentation of birchwood xylan to ethanol by a recombinant *S. cerevisiae* strain containing an integrated D-xylose-utilizing pathway. The fermentation medium was prepared in an anaerobic chamber with 1% yeast extract, 2% peptone, 1% birchwood xylan, 0.001% ergosterol, and 0.042% Tween 80. Cells were resuspended to an OD_{600} of ~50. The experiments were carried out anaerobically with serum bottles at 30°C at 250 rpm. All the data were obtained from triplicate experiments, and the averages and standard deviations are plotted.

abilities in xylose medium (2% xylose in SC dropout medium) to eliminate possible metabolic influences when minihemicellulosomes were expressed in yeast cells (see Fig. S4 in the supplemental material). Strain HZ3001 exhibited a slightly higher growth rate than strain HZ3345. Further direct fermentation from xylan to ethanol was performed anaerobically with 10 g/liter birchwood xylan. As shown in Fig. 6, the ethanol concentration increased as the residual total sugar was consumed. After 80 h, the ethanol titer reached approximately ~0.95 g/liter, while the residual total sugar level decreased to ~6.88 g/liter. The highest yield was 0.31 g of ethanol produced per g of birchwood xylan consumed. The production of ethanol was not detected in the control strain.

DISCUSSION

In this study, yeast surface display was used to engineer *S. cerevisiae* strains with minihemicellulosomes anchored on the cell surface (Fig. 1). The extracellular surface display allows the detection of labeled antigen-antibody interactions by flow cytometry. By labeling different proteins with different antigens, we can quickly assay each component in the minihemicellulosomes at one time, which significantly reduces time and labor.

Similar to the minicellulosome, an engineered minihemicellulosome is also a multienzyme complex including several assembled modules (Fig. 1). A previous study reported the codisplay of an endoxylanase (XynII) and a β-xylosidase (XylA) as individual fusion proteins with the C-terminal-half region of a-agglutinin (21). However, there was no miniscaffoldin, and the enzymes were distributed randomly on the cell surface. An enzyme-enzyme synergy between XynII and XylA was shown but only in a 3-h reaction. In our study, the minihemicellulosomes were more stable and could readily hydrolyze xylan for days. Another previously reported example used the purified multimeric hemicellulase to synergistically degrade complex polysaccharides, which involved only a carbohydrate-binding domain without the cohesin-dockerin high-affinity interactions (12). Neither of the previous studies could illustrate the structure of the hemicellulosome and its responsible mechanisms in the hydrolysis process. Similar to a protuberance-like surface structure in native cellulolytic bacteria (5), the miniscaffoldin serves as a base to establish the interactions between a cell and enzymes. Meanwhile, the critical elements in the multienzyme complex to solubilize a cellulosic polymer have been explored (36, 54). In this study, a miniscaffoldin was stably anchored to the cell wall and was used to incorporate three different xylanases to form a minihemicellulosome.

In previous studies, the effect of target xylanases was simply determined by an enzyme cocktail, which only quantitatively increases the enzyme variety and dosage (17, 46). In this study, a proximity effect of xylanases was brought into consideration with two types of miniscaffoldins, CipA3 and CipA1. This showed that the enzyme proximity synergy might play a role, especially in the case of the enzyme AbfB. Only when AbfB was brought close to XynII and XlnD (CipA3-based minihemicellulosomes) did it exhibit synergism (Fig. 5). Otherwise, AbfB could hardly expose more nonreducing ends for XynII to attack, resulting in little enhancement of reducing sugar production (CipA1-based minihemicellulosomes) (Fig. 5). In addition to potential enzyme-enzyme synergy and enzyme proximity synergy, the enhanced hydrolysis rate of arabinoxylan observed for the quaternary trifunctional minihemicellulosome might be due to an overall effect caused by the enzyme source, glycosylation, display efficiency, cohesin-dockerin interaction affinity, and so on. All these issues should be addressed in order to clarify the bottlenecks in minihemicellulosome construction.

The observed synergy is not necessarily positively proportional to the number of xylanases. As in the case of the substrate birchwood xylan, which contains fewer substitutions of arabinose, the CipA3-XynII-XlnD strain can liberate more reducing sugars than the CipA3-XynII-AbfB-XlnD strain (Fig. 4B). This finding suggested that the design of a minihemicellulosome to achieve a maximum hydrolysis rate is also dependent on the compositions of xylan. A full understanding of the synergistic action of xylanases in the hemicellulosome could lead to the cost-effective saccharification of naturally derived biomass and thus overcome a major barrier to the industrial production of biofuel.

In addition, several future studies will be taken into consideration. First, such a platform can be applied to realize the synergy between cellulases and xylanases by readily swapping the enzymes through the DNA assembler method (44), which allows the fast assembly of genes in a one-step manner. By creating a super cellulosome/hemicellulosome, the simultaneous assimilation of C_6 and C_5 polysaccharides may be realized. A recent study reported a recombinant *S. cerevisiae* strain codisplaying an endoxylanase, a xylosidase, and a glucosidase, which exhibited a high ethanol yield of 0.41 g/g from a rice straw hydrolysate (41). Second, the strength of the cohesin-dockerin interactions in docS and docA have not yet been compared in this work, as the dockerin and the corresponding xylanase were designated as one configuration. The uncontrolled expression and arrangement of hemicellulosomal components would lead to some clonal variations. To address this issue, one strategy is to construct designer hemicellulosomes, in which the cohesin and dockerin are specifically paired (30, 37) so that the hemicellulosomal components can be expressed in an optimized proportion rather than unbalanced. Another strategy is to integrate the heterologous xylanase genes into chromosomal DNA with multiple copies by cocktail δ-integration, which can simultaneously control the expression level of each xylanase and

their ratios (41, 53). Third, direct fermentation was attempted only with bifunctional minihemicellulosomes and one integrated xylose-utilizing pathway to avoid a potential metabolic burden on the yeast cells. Further simultaneous saccharification and fermentation of arabinoxylan are feasible by transforming trifunctional hemicellulosomes into an *S. cerevisiae* strain that contains chromosomally integrated xylose- and arabinose-utilizing pathways, which can then be applied to complete the saccharification of other raw materials.

In conclusion, upon the incorporation of three complementary xylan-degrading xylanases into the same miniscaffoldin, an enhanced degradation of arabinoxylan was obtained. The main advantages of such a recombinant yeast strain may be the high tolerance to toxicities and the elimination of the purification step, which reduce the overall cost of production of a target protein in industrial applications. A CBP strategy was achieved in this study, which could simultaneously hydrolyze xylan into xylose and ferment xylose into ethanol. Further investigations are required to improve the xylan degradation ability of the CBP strain, since the residual total sugar concentration reached a plateau after 80 h (Fig. 6). For the complete degradation and saccharification of xylan, other critical xylanases might also be needed.

ACKNOWLEDGMENTS

This work is supported by the Centennial Endowed Chair Fund of the Department of Chemical and Biomolecular Engineering at the University of Illinois at Urbana-Champaign, the East China University of Science and Technology, and the Chinese Scholarship Council (file no. 2008674002).

REFERENCES

1. **Ahmed S, Riaz S, Jamil A.** 2009. Molecular cloning of fungal xylanases: an overview. Appl. Microbiol. Biotechnol. **84**:19–35.
2. **Bayer EA, Lamed R.** 1986. Ultrastructure of the cell surface cellulosome of *Clostridium thermocellum* and its interaction with cellulose. J. Bacteriol. **167**:828–836.
3. **Bayer EA, Lamed R, Himmel ME.** 2007. The potential of cellulases and cellulosomes for cellulosic waste management. Curr. Opin. Biotechnol. **18**:237–245.
4. **Bayer EA, Morag E, Lamed R.** 1994. The cellulosome—a treasure-trove for biotechnology. Trends Biotechnol. **12**:379–386.
5. **Bayer EA, Shimon LJ, Shoham Y, Lamed R.** 1998. Cellulosomes—structure and ultrastructure. J. Struct. Biol. **124**:221–234.
6. **Beguin P, Alzari PM.** 1998. The cellulosome of *Clostridium thermocellum*. Biochem. Soc. Trans. **26**:178–185.
7. **Beguin P, Cornet P, Aubert JP.** 1985. Sequence of a cellulase gene of the thermophilic bacterium *Clostridium thermocellum*. J. Bacteriol. **162**:102–105.
8. **Cho HY, Yukawa H, Inui M, Doi RH, Wong SL.** 2004. Production of minicellulosomes from *Clostridium cellulovorans* in *Bacillus subtilis* WB800. Appl. Environ. Microbiol. **70**:5704–5707.
9. **Crous JM, Pretorius IS, van Zyl WH.** 1996. Cloning and expression of the alpha-L-arabinofuranosidase gene (ABF2) of *Aspergillus niger* in *Saccharomyces cerevisiae*. Appl. Microbiol. Biotechnol. **46**:256–260.
10. **Dodd D, Cann IK.** 2009. Enzymatic deconstruction of xylan for biofuel production. Glob. Change Biol. Bioenergy **1**:2–17.
11. **Doi RH, Kosugi A.** 2004. Cellulosomes: plant-cell-wall-degrading enzyme complexes. Nat. Rev. Microbiol. **2**:541–551.
12. **Fan Z, et al.** 2009. Multimeric hemicellulases facilitate biomass conversion. Appl. Environ. Microbiol. **75**:1754–1757.
13. **Fujita Y, Ito J, Ueda M, Fukuda H, Kondo A.** 2004. Synergistic saccharification, and direct fermentation to ethanol, of amorphous cellulose by use of an engineered yeast strain codisplaying three types of cellulolytic enzyme. Appl. Environ. Microbiol. **70**:1207–1212.
14. **Fujita Y, et al.** 2002. Construction of whole-cell biocatalyst for xylan degradation through cell-surface xylanase display in *Saccharomyces cerevisiae*. J. Mol. Catal. B Enzym. **17**:189–195.
15. **Gerngross UT, Romaniec MP, Kobayashi T, Huskisson NS, Demain AL.** 1993. Sequencing of a *Clostridium thermocellum* gene (*cipA*) encoding the cellulosomal SL-protein reveals an unusual degree of internal homology. Mol. Microbiol. **8**:325–334.
16. **Girio FM, et al.** 2010. Hemicelluloses for fuel ethanol: a review. Bioresour. Technol. **101**:4775–4800.
17. **Hashimoto T, Nakata Y.** 2003. Synergistic degradation of arabinoxylan with alpha-L-arabinofuranosidase, xylanase and beta-xylosidase from soy sauce koji mold, Aspergillus oryzae, in high salt condition. J. Biosci. Bioeng. **95**:164–169.
18. **Himmel ME, et al.** 2007. Biomass recalcitrance: engineering plants and enzymes for biofuels production. Science **315**:804–807.
19. **Hyeon JE, et al.** 2010. Production of minicellulosomes from *Clostridium cellulovorans* for the fermentation of cellulosic ethanol using engineered recombinant *Saccharomyces cerevisiae*. FEMS Microbiol. Lett. **310**:39–47.
20. **Jiang Z, et al.** 2006. Subunit composition of a large xylanolytic complex (xylanosome) from *Streptomyces olivaceoviridis* E-86. J. Biotechnol. **126**:304–312.
21. **Katahira S, Fujita Y, Mizuike A, Fukuda H, Kondo A.** 2004. Construction of a xylan-fermenting yeast strain through codisplay of xylanolytic enzymes on the surface of xylose-utilizing *Saccharomyces cerevisiae* cells. Appl. Environ. Microbiol. **70**:5407–5414.
22. **Kohring S, Wiegel J, Mayer F.** 1990. Subunit composition and glycosidic activities of the cellulase complex from *Clostridium thermocellum* JW20. Appl. Environ. Microbiol. **56**:3798–3804.
23. **Kondo A, Tanaka T, Hasunuma T, Ogino C.** 2010. Applications of yeast cell-surface display in bio-refinery. Recent Pat. Biotechnol. **4**:226–234.
24. **La Grange DC, Pretorius IS, Claeyssens M, van Zyl WH.** 2001. Degradation of xylan to D-xylose by recombinant *Saccharomyces cerevisiae* coexpressing the *Aspergillus niger* beta-xylosidase (xlnD) and the *Trichoderma reesei* xylanase II (xyn2) genes. Appl. Environ. Microbiol. **67**:5512–5519.
25. **La Grange DC, Pretorius IS, van Zyl WH.** 1996. Expression of a *Trichoderma reesei* beta-xylanase gene (XYN2) in *Saccharomyces cerevisiae*. Appl. Environ. Microbiol. **62**:1036–1044.
26. **Li S, et al.** 2010. Overcoming glucose repression in mixed sugar fermentation by co-expressing a cellobiose transporter and a beta-glucosidase in *Saccharomyces cerevisiae*. Mol. Biosyst. **6**:2129–2132.
27. **Lynd LR, van Zyl WH, McBride JE, Laser M.** 2005. Consolidated bioprocessing of cellulosic biomass: an update. Curr. Opin. Biotechnol. **16**:577–583.
28. **Ma H, Kunes S, Schatz PJ, Botstein D.** 1987. Plasmid construction by homologous recombination in yeast. Gene **58**:201–216.
29. **Margolles-Clark E, Tenkanen M, Nakari-Setala T, Penttila M.** 1996. Cloning of genes encoding alpha-L-arabinofuranosidase and beta-xylosidase from *Trichoderma reesei* by expression in *Saccharomyces cerevisiae*. Appl. Environ. Microbiol. **62**:3840–3846.
30. **Mechaly A, et al.** 2001. Cohesin-dockerin interaction in cellulosome assembly: a single hydroxyl group of a dockerin domain distinguishes between nonrecognition and high affinity recognition. J. Biol. Chem. **276**:9883–9888.
31. **Mingardon F, et al.** 2005. Heterologous production, assembly, and secretion of a minicellulosome by *Clostridium acetobutylicum* ATCC 824. Appl. Environ. Microbiol. **71**:1215–1222.
32. **Morais S, et al.** 2010. Cellulase-xylanase synergy in designer cellulosomes for enhanced degradation of a complex cellulosic substrate. mBio **1**(5):e00285–10. doi:10.1128/mBio.00285-10.
33. **Morais S, et al.** 2010. Contribution of a xylan-binding module to the degradation of a complex cellulosic substrate by designer cellulosomes. Appl. Environ. Microbiol. **76**:3787–3796.
34. **Morais S, et al.** 2011. Assembly of xylanases into designer cellulosomes promotes efficient hydrolysis of the xylan component of a natural recalcitrant cellulosic substrate. mBio **2**(6):e00233–11. doi:10.1128/mBio.e00233-11.
35. **Nair NU, Zhao H.** 2012. Mutagenic inverted repeats assisted genome engineering (MIRAGE) in *Saccharomyces cerevisiae*: deletion of *gal7*. Methods Mol. Biol. **834**:63–73.
36. **Olson DG, et al.** 2010. Deletion of the Cel48S cellulase from *Clostridium thermocellum*. Proc. Natl. Acad. Sci. U. S. A. **107**:17727–17732.
37. **Pages S, et al.** 1997. Species-specificity of the cohesin-dockerin interaction between *Clostridium thermocellum* and *Clostridium cellulolyticum*: prediction of specificity determinants of the dockerin domain. Proteins **29**:517–527.

38. **Polizeli ML, et al.** 2005. Xylanases from fungi: properties and industrial applications. Appl. Microbiol. Biotechnol. **67**:577–591.
39. **Sabathe F, Soucaille P.** 2003. Characterization of the CipA scaffolding protein and *in vivo* production of a minicellulosome in *Clostridium acetobutylicum*. J. Bacteriol. **185**:1092–1096.
40. **Saha BC.** 2003. Hemicellulose bioconversion. J. Ind. Microbiol. Biotechnol. **30**:279–291.
41. **Sakamoto T, Hasunuma T, Hori Y, Yamada R, Kondo A.** 29 June 2011, posting date. Direct ethanol production from hemicellulosic materials of rice straw by use of an engineered yeast strain codisplaying three types of hemicellulolytic enzymes on the surface of xylose-utilizing *Saccharomyces cerevisiae* cells. J. Biotechnol. [Epub ahead of print.] doi:10.1016/j.jbiotec.2011.06.025.
42. **Sanchez OJ, Cardona CA.** 2008. Trends in biotechnological production of fuel ethanol from different feedstocks. Bioresour. Technol. **99**:5270–5295.
43. **Service RF.** 2007. Cellulosic ethanol. Biofuel researchers prepare to reap a new harvest. Science **315**:1488–1491.
44. **Shao Z, Zhao H, Zhao H.** 2009. DNA assembler, an *in vivo* genetic method for rapid construction of biochemical pathways. Nucleic Acids Res. **37**:e16.
45. **Shimon LJ, et al.** 1997. A cohesin domain from *Clostridium thermocellum*: the crystal structure provides new insights into cellulosome assembly. Structure **5**:381–390.
46. **Sorensen HR, Pedersen S, Jorgensen CT, Meyer AS.** 2007. Enzymatic hydrolysis of wheat arabinoxylan by a recombinant "minimal" enzyme cocktail containing beta-xylosidase and novel endo-1,4-beta-xylanase and alpha-L-arabinofuranosidase activities. Biotechnol. Prog. **23**:100–107.
47. **Tsai SL, Oh J, Singh S, Chen R, Chen W.** 2009. Functional assembly of minicellulosomes on the *Saccharomyces cerevisiae* cell surface for cellulose hydrolysis and ethanol production. Appl. Environ. Microbiol. **75**:6087–6093.
48. **van Zyl WH, Lynd LR, den Haan R, McBride JE.** 2007. Consolidated bioprocessing for bioethanol production using *Saccharomyces cerevisiae*. Adv. Biochem. Eng. Biotechnol. **108**:205–235.
49. **Wang WK, Kruus K, Wu JH.** 1993. Cloning and DNA sequence of the gene coding for *Clostridium thermocellum* cellulase Ss (CelS), a major cellulosome component. J. Bacteriol. **175**:1293–1302.
50. **Wen F, Nair NU, Zhao H.** 2009. Protein engineering in designing tailored enzymes and microorganisms for biofuels production. Curr. Opin. Biotechnol. **20**:412–419.
51. **Wen F, Sun J, Zhao H.** 2010. Yeast surface display of trifunctional minicellulosomes for simultaneous saccharification and fermentation of cellulose to ethanol. Appl. Environ. Microbiol. **76**:1251–1260.
52. **Wood TM, Bhat KM.** 1988. Methods for measuring cellulase activities. Method Enzymol. **160**:87–112.
53. **Yamada R, et al.** 2010. Cocktail delta-integration: a novel method to construct cellulolytic enzyme expression ratio-optimized yeast strains. Microb. Cell Fact. **9**:32.
54. **Zverlov VV, Klupp M, Krauss J, Schwarz WH.** 2008. Mutations in the scaffoldin gene, cipA, of *Clostridium thermocellum* with impaired cellulosome formation and cellulose hydrolysis: insertions of a new transposable element, IS1447, and implications for cellulase synergism on crystalline cellulose. J. Bacteriol. **190**:4321–4327.